



Contents lists available at ScienceDirect

Bioorganic & Medicinal Chemistry Letters

journal homepage: www.elsevier.com/locate/bmcl

3-Benzyl-1,3-oxazolidin-2-ones as mGluR2 positive allosteric modulators: Hit-to-lead and lead optimization

Allen J. Duplantier^{a,*}, Ivan Efremov^{b,*}, John Candler^b, Angela C. Doran^d, Alan H. Ganong^c, Jessica A. Haas^d, Ashley N. Hanks^c, Kenneth G. Kraus^a, John T. Lazzaro Jr.^c, Jiemin Lu^a, Noha Maklad^a, Sheryl A. McCarthy^c, Theresa J. O'Sullivan^b, Bruce N. Rogers^a, Judith A. Siuciak^{c,†}, Douglas K. Spracklin^d, Lei Zhang^a

^a CNS Chemistry, Pfizer Global Research and Development, Eastern Point Road, Groton, CT 06340, USA

^b Lead Generation Group, Pfizer Global Research and Development, Eastern Point Road, Groton, CT 06340, USA

^c Department of Neuroscience, Pfizer Global Research and Development, Eastern Point Road, Groton, CT 06340, USA

^d Department of Pharmacokinetics and Drug Metabolism, Pfizer Global Research and Development, Eastern Point Road, Groton, CT 06340, USA

ARTICLE INFO

Article history:

Received 6 January 2009

Revised 9 March 2009

Accepted 10 March 2009

Available online 14 March 2009

Keywords:

mGluR2

Positive allosteric modulator

Carbamate

Schizophrenia

ABSTRACT

The discovery, synthesis and SAR of a novel series of 3-benzyl-1,3-oxazolidin-2-ones as positive allosteric modulators (PAMs) of mGluR2 is described. Expedient hit-to-lead work on a single HTS hit led to the identification of a ligand-efficient and structurally attractive series of mGluR2 PAMs. Human microsomal clearance and suboptimal physicochemical properties of the initial lead were improved to give potent, metabolically stable and orally available mGluR2 PAMs.

© 2009 Elsevier Ltd. All rights reserved.

Metabotropic glutamate type 2 receptors (mGluR2) are G-protein coupled receptors¹ that are localized presynaptically on glutamate neurons and modulate neurotransmitter release.² Known mGluR2 agonists also have agonist activity at mGluR3 receptors which are the closest mGluR family member with a high degree of homology at the agonist binding site.^{1,3} Mixed mGluR2/3 agonists have been shown to be effective in a variety of preclinical animal models of anxiety^{4,5} and schizophrenia,^{5–7} and recently, LY2140023 was reportedly active in a phase IIb clinical trial against the positive and negative symptoms of schizophrenia.⁸ Positive allosteric modulators (PAMs) of mGluR2 have been reported by others in the literature⁹ and most recently by our group.¹⁰ PAMs may offer an advantage over agonists of mGluR2 as potentially selective tools to gain a clear understanding of the mGluR2 subtype, and allow for chemotype diversity without the structural restrictions imposed by the agonist binding pocket.¹¹ Additional advantages of PAMs may include less receptor desensitization,¹² and upregulation of receptor-mediated effects only when the

receptor is stimulated by either naturally released or exogenous agonist. This latter point, however, may complicate the interpretation of in vivo efficacy data of mGluR2 PAMs due to an inability to compare the glutamate tone at the synapse of animal models with that in patients. Herein, we describe the identification, SAR development and optimization of a novel class of mGluR2 modulators identified by high-throughput screening (HTS) of our compound file.

Choosing an appropriate starting point from a variety of hits identified by HTS campaigns is a critical stage in the drug discovery process. Not surprisingly, the pharmaceutical industry at large has paid significant attention to the development of a more efficient and robust hit-to-lead process.¹³ Two critical stages in this process are the hit assessment (identity and sample integrity confirmation along with physicochemical properties assessment) and hit validation (re-assay and possibly resynthesis) steps.

Our approach to identification of mGluR2 PAM lead matter involved an HTS campaign and some of the results from that effort have recently been reported.¹⁰ The triage of hit structures drew our attention to a unique chemotype represented by structure **1** (Fig. 1), an in-house compound that was structurally distinct from known mGluR2 PAMs.^{9,10}

Calculated properties of **1** (MW, log*P*, solubility, polar surface area) coupled with synthetic enablement (Fig. 1) looked promising, but the analytical evaluation of the original sample by ¹H NMR and

* Corresponding authors. Tel.: +1 860 441 6009 (A.J.D.); tel.: +1 860 441 686 1373 (I.E.).

E-mail addresses: allen.j.duplantier@pfizer.com (A.J. Duplantier), ivan.efremov@pfizer.com (I. Efremov).

† Present address: The Biomarkers Consortium, Foundation for the NIH, Bethesda, MD, USA.

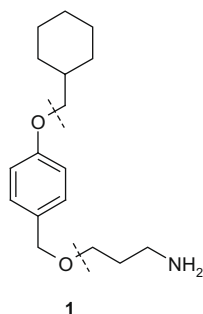
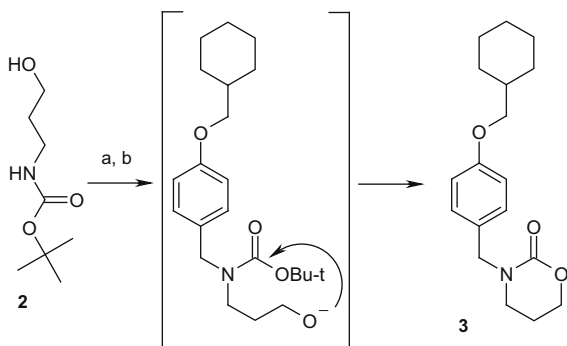


Figure 1. Presumed structure of the HTS hit **1** and potential synthetic disconnections.

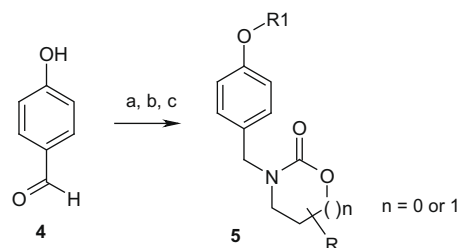


Scheme 1. Proposed rationale for formation of compound **3** responsible for mGluR2 activity in the HTS hit. Reagents: (a) NaH, DMF; (b) (*para*-cyclohexyl-methoxy)benzyl chloride, DMF.

LC–MS revealed the presence of only trace amounts of **1**. Indeed, resynthesis and evaluation of the authentic compound **1** confirmed that no desired pharmacological activity resided in this chemical structure. Additional purification of the active batch followed by a battery of analytical methods (^1H and ^{13}C NMR, HRMS, UV, IR), allowed us to arrive at structure **3** as the active component, and this structure was confirmed by X-ray crystallography (data not shown). This result prompted us to investigate in detail the synthetic route used for the original synthesis of compound **1**. The likely explanation for the formation of **3** appears to be an inadvertent use of an excess of base during deprotonation of the Boc-protected amino alcohol **2** (Scheme 1). The resulting dianion would cause N-alkylation of **2** with *para*-(cyclohexyl methoxy)benzyl chloride rather than the intended O-alkylation. The subsequent spontaneous cyclization of the intermediate would then lead to the observed compound **3**. We were pleased to see that upon re-assay of the purified sample of **3**, potent mGluR2 PAM activity ($\text{EC}_{50} = 117 \text{ nM}$) was observed.

At this stage our attention shifted to the assessment of the structure **3** as a starting point for lead identification. The calculated and measured *in vitro* properties of **3** (*cLogP*, polar surface area, MDCK,¹⁴ MDR¹⁵) were predictive of good brain penetration, and its potency and low molecular weight suggested good ligand efficiency.^{16,17} Among a variety of synthetic routes that could be used for synthesis of this chemotype, we chose an alkylation/reductive amination sequence followed by carbamate formation as represented in Scheme 2. The advantages of this route included amenability toward parallel synthesis coupled with ready availability of diverse precursors, thus enabling efficient SAR development.

While a virtual library comprising several thousands of products could be enumerated using available starting materials, our goal was to reach decision making on this chemotype in one iteration of



Scheme 2. Reagents and conditions: (a) R^1OH , Ph_3P , DBAD, toluene, rt; (b) aminoalcohol, $\text{NaBH}(\text{OAc})_3$, 1,2-dichloroethane, rt; (c) carbonyl diimidazole, 1,2-dichloroethane, 80°C , 2 h.

parallel synthesis. The key questions to answer were SAR responsiveness and an ability to increase potency while remaining in the chemical space of CNS drugs.¹⁸ With this in mind, the key criteria used for library design were systematic structural changes in the scaffold, molecular weight, lipophilicity, polar surface area, and a score from a proprietary *in silico* model assessing potential for P-gp efflux. To methodically evaluate these properties from a structural perspective, our main parameters for the selection of library precursors became: size, degree of saturation and polarity of ‘head’ substituents (R^1 in Scheme 2); linker length in R^1 ; ring size of the ‘tail’ (carbamate) substituents; polarity and placement of additional substitution on the cyclic carbamate ring. Of particular note was an attempt to introduce polarity in both head and tail parts of the scaffold to balance the lipophilic nature of the hit structure **3**. The library was produced with 92% success rate and provided timely SAR information used for decision making in this mGluR2 hit series. Some observations are highlighted in Table 1.

The prepared set of analogs allowed for a confident assessment of the lead potential for this series and highlighted key areas for improvement. It was observed that the SAR was additive between substituents.¹⁹ From a potency perspective, we found the SAR to be very responsive. The optimal linker between ether oxygen and the ring was a single-carbon chain, preferably branched (compounds **6**, **7**, **10** and **11**, Table 1). Ring size of the carbamate substituent had an interesting effect on activity – five-membered carbamate with substitution next to oxygen was optimal with unsubstituted five- and six-membered carbamates being inferior (compounds **3**, **7** and **14**). Substitution next to nitrogen in the five-membered carbamates was clearly detrimental and, while some substitution on the six-membered carbamates was tolerated, it still resulted in loss of potency. Compound **13** illustrates one possible avenue for polarity modulation. It is worth noting that a corresponding *N*-methyl piperidine derivative was not active at $10 \mu\text{M}$ (data not shown). As shown by the two diastereomeric isomers of **6** (compounds **8** and **17**), greater desired activity resided within the *R*-configuration of the stereogenic center on the carbamate ring.

Compound **17** (Fig. 2) displayed *in vitro* ADME properties predictive of good brain penetration (MDCK AB $>10 \times 10^{-6} \text{ cm/s}$ and MDR BA/AB <2.5),²⁰ and this was confirmed *in vivo* in the mouse [brain/plasma ratio = 3.0 (32 mg/kg, s.c.)]. In addition, **17** showed no significant CYP inhibition²¹ and dofetilide displacement assay data²² suggested a low potential for hERG channel inhibition. However, although **17** was a potent mGluR2 PAM ($\text{EC}_{50} = 5 \text{ nM}$) with good brain penetration, it also had high *in vitro* human liver microsomal clearance (14.7 mL/min/kg), a high *cLogP* (5.12) and a melting point (MP) below room temperature making it difficult to manufacture on a kg scale. Our strategy to address these issues was to introduce an ionizable center and/or increase the polarity, and to replace the alkylether moiety with metabolically stable groups such as substituted aryls while retaining low molecular weight (<400).

Amino analogs **20** and **21** were prepared by reductive amination of aldehydes **18a** and **18b**, respectively, with (*R*)-(–)-1-amino-2-

Table 1
Functional activities and human microsomal clearance data of representative mGluR2 PAMs (general structure 5)

| Compound | R ¹ | carbamate | mGluR2 EC ₅₀ (nM) ^a | h-CL _h (mL/min/kg) ^b |
|----------------|----------------|-----------|---|--|
| 6 ^c | | | 7.9 | 16 |
| 7 | | | 15 | 9.9 |
| 8 | | | 22.1 | 13.6 |
| 9 | | | 75 | 10 |
| 3 | | | 117 | 9.1 |
| 10 | | | 203 | <5.3 |
| 11 | | | 236 | 14 |
| 12 | | | 262 | <5.3 |
| 13 | | | 384 | 14.5 |
| 14 | | | 590 | <5.3 |
| 15 | | | >10,000 | <5.3 |
| 16 | | | >10,000 | ND ^d |

^a EC₅₀ values obtained from mGluR2 receptor transfected HEK cell line using FLIPR method in the presence of glutamate (EC₁₀₋₂₀); means of at least three experiments; an EC₅₀ value >10,000 indicates that no curve was noted in the dose–response up to 10 μM.

^b Predicted hepatic clearance (CL_h) from human liver microsomal stability assay.

^c Mixture of diastereomeric pairs.

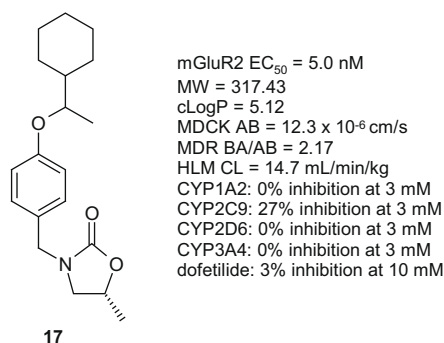
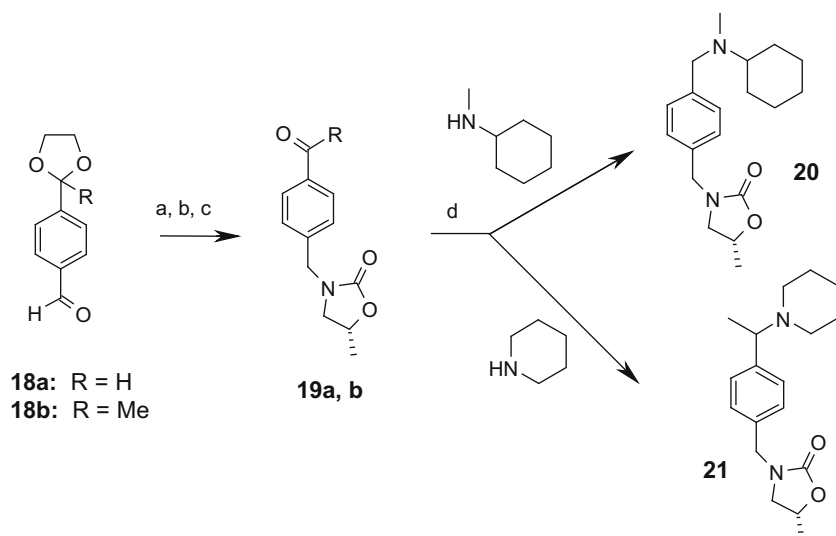


Figure 2. In vitro ADME profiling of a representative hit follow-up structure.

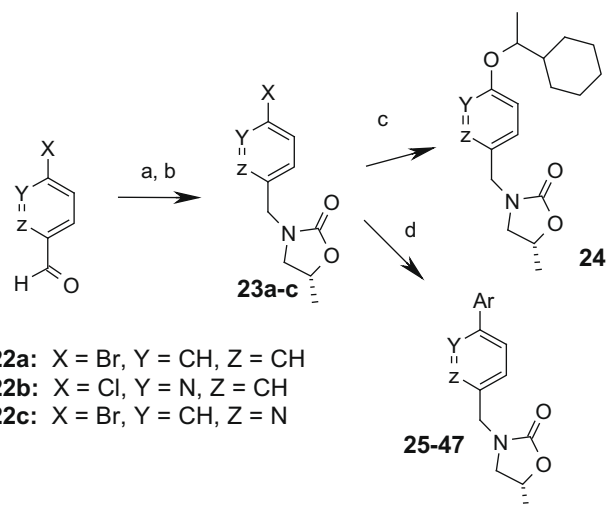
propanol followed by carbamate cyclization with carbonyl diimidazole, subsequent deprotection of the dioxolane ring (to give **19a** and **b**), and then reductive amination with either cyclohexyl methylamine or piperidine (Scheme 3). The cyclic carbamate moiety of intermediates **23a–c** were prepared in a similar manner from aldehydes **22a–c** as described in Scheme 4. Pyridyl analog **24** was synthesized by arylation of 1-cyclohexylethanol with **23b**. Suzuki coupling of the appropriate arylboronic acid and arylhalide (**23a–c**) provided biaryl analogs **25–47**, as well as aldehyde intermediates **48a** and **b** (see Table 2 for definitions of Ar, Y and Z). Reductive amination of **48a** and **b** with dimethylamine afforded amino analogs **49a** and **b**, respectively (Scheme 5).

Efforts to address the high CL and low MP entailed the introduction of a basic amine into the cycloalkyl moiety of **17**. To that end, amino compounds **20** and **21** reduced cLogP and in vitro metabolic clearance, and provided a salt handle. However, the introduction of polar functionality into this part of the molecule proved to be detrimental to mGluR2 activity (see Table 2). Substitution of the central phenyl ring of compound **17** with a pyridyl group (**24**) had a less dramatic effect on potency (EC_{50} = 88 nM), but did not improve CL.

As an alternative strategy to reduce CL and increase the MP, we replaced the alkylether moiety of **17** with phenyl²³ (**25**). Not surprisingly, **25** was also metabolically labile, presumably due to oxidation around the phenyl rings, so we attempted to block metabolism by systematically substituting F, Cl and OMe groups around the terminal phenyl ring (compounds **26–34**, Table 2). The interesting SAR that emerged from this exercise was the discovery that



Scheme 3. Reagents and conditions: (a) (*R*)-(-)-1-amino-2-propanol, Na(OAc)₃BH, CH₂Cl₂, 18 h, rt; (b) carbonyl diimidazole, THF, 80 °C, 4 h; (c) sulfuric acid (cat.), acetone, reflux, 32%; (d) Na(OAc)₃BH, CH₂Cl₂, 18 h, rt.



Scheme 4. Reagents and conditions: (a) (*R*)-(-)-1-amino-2-propanol, Na(OAc)₃BH, CH₂Cl₂, 18 h, rt; (b) carbonyl diimidazole, THF, 80 °C, 4 h; (c) 1-cyclohexylethanol, potassium *tert*-butoxide, THF, 120 °C (microwave), 10 min, 20%; (d) ArB(OH)₂, Pd(PPh₃)₄, Na₂CO₃, EtOH, 120 °C (microwave), 5 min.

ortho-substitution (**26**, **29** and **32**) improved potency and *para*-substitution (**28** and **31**) lowered clearance. The high CL observed with the 4-methoxy analog **34** was likely due to metabolic demethylation, as the corresponding ethoxy (**36**) and trifluoromethoxy (**37**) analogs were stable in the presence of human liver microsomes. The most interesting compounds identified were the di-substituted analogs **38–40**, where the substituent at the 4-position blocked metabolism and the second substituent appeared to improve potency. Compounds **38–40** were obtained in solid form, but their low MPs (<90 °C) and low aqueous solubility were difficult to address due to the lack of an ionizable center from which to prepare alternative salt forms. To that end, attempts to introduce heterocyclic (**41–47**) and amino (**49a** and **b**) functionality led to metabolically stable analogs with improved solubility and lower cLogP (<4), but once again with reduced mGluR2 potency.

Selected compounds were profiled further for selectivity against a panel of CNS receptors (data not shown), and compound **40** was found to have moderate 5-HT_{2A} activity (K_i = 323 nM). Interestingly, only biaryl analogs with fluoro-substitution had

Table 2
Functional activities, in vitro human microsomal clearance data and *cLogP* values of representative mGluR2 PAMs

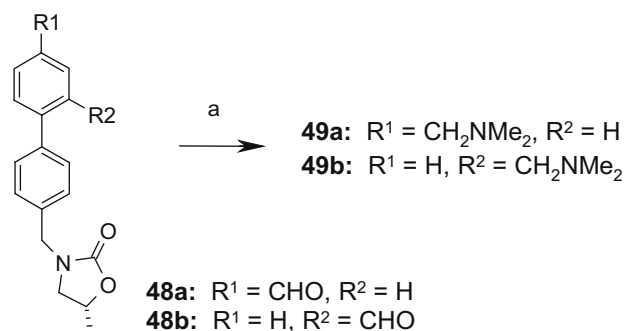
| Entry | Y | Z | Ar | mGluR2 EC ₅₀ ^a (nM) | h-CL _h ^b (mL/min/kg) | <i>cLogP</i> ^d |
|-------|----|----|------------------------------------|---|--|---------------------------|
| 20 | — | — | — | >10,000 | 8.1 | 4.11 |
| 21 | — | — | — | >10,000 | <5.3 | 3.58 |
| 24 | N | CH | — | 88 | 15.4 | 4.52 |
| 25 | CH | CH | Phenyl | 142 | >18.7 | 4.13 |
| 26 | CH | CH | 2-Fluorophenyl | 35 | >18.7 | 4.27 |
| 27 | CH | CH | 3-Fluorophenyl | 280 | 18.1 | 4.27 |
| 28 | CH | CH | 4-Fluorophenyl | 84 | 5.7 | 4.27 |
| 29 | CH | CH | 2-Chlorophenyl | 28 | >18.7 | 4.59 |
| 30 | CH | CH | 3-Chlorophenyl | 158 | ND ^c | 4.84 |
| 31 | CH | CH | 4-Chlorophenyl | 76 | 8.4 | 4.84 |
| 32 | CH | CH | 2-Methoxyphenyl | 41 | >18.7 | 3.49 |
| 33 | CH | CH | 3-Methoxyphenyl | 275 | >18.7 | 4.05 |
| 34 | CH | CH | 4-Methoxyphenyl | 53 | 18.6 | 4.05 |
| 35 | CH | CH | 2-Ethoxyphenyl | 26 | >18.7 | 4.02 |
| 36 | CH | CH | 4-Ethoxyphenyl | 97 | <5.3 | 4.58 |
| 37 | CH | CH | 4-Trifluoro-methoxyphenyl | 183 | <5.3 | 5.16 |
| 38 | CH | CH | 3-Chloro-4-fluorophenyl | 30 | 8.3 | 4.98 |
| 39 | CH | CH | 2-Fluoro-4-trifluoro-methoxyphenyl | 32 | <5.3 | 5.44 |
| 40 | CH | CH | 2,4-Difluorophenyl | 70 | 7.3 | 4.42 |
| 41 | CH | CH | 4-Pyridyl | 4790 | 13.2 | 2.63 |
| 42 | CH | CH | 3-Pyridyl | 7550 | <5.3 | 2.63 |
| 43 | CH | CH | Pyrimidin-5-yl | 4380 | ND | 1.68 |
| 44 | N | CH | 2-Fluoro-4-trifluoro-methoxyphenyl | 380 | <5.3 | 4.19 |
| 45 | N | CH | 3-Chloro-4-fluorophenyl | 595 | <5.3 | 3.72 |
| 46 | N | CH | 2,4-Difluorophenyl | 3400 | <5.3 | 3.15 |
| 47 | CH | N | 2,4-Difluorophenyl | 1800 | <5.3 | 2.94 |
| 49a | — | — | — | 3060 | ND | 3.96 |
| 49b | — | — | — | 6360 | 9.7 | 3.66 |

^a EC₅₀ values obtained from rat mGluR2 receptor transfected HEK cell line using FLIPR method in the presence of glutamate (EC_{10–20}); means of at least three experiments.

^b Predicted hepatic clearance from human liver microsomal stability assay.

^c ND, not determined.

^d In silico calculation of log*P*.



Scheme 5. Reagents and conditions: (a) Dimethylamine, Na(OAc)₃BH, CH₂Cl₂, 18 h, rt.

sub-micromolar activity against 5-HT_{2A}, as compounds containing any larger group such as chloro (**38**) or trifluoromethoxy (**39**), or

Table 4
Methamphetamine induced locomotor activity in mice^a

| Compounds | MED ^b (mg/kg, sc) | [Brain] (ng/g) | [Plasma] (ng/mL) | B/P | Fu _p ; Fu _b ^c | [Plasma] _{free} ; [brain] _{free} ^d (nM) |
|-----------|------------------------------|----------------|------------------|-----|--|--|
| LY354740 | 0.01 | — | — | — | — | — |
| 38 | 10 | 2750 | 750 | 3.7 | 0.014; 0.004 | 33; 34 |
| 40 | 10 | 2230 | 1070 | 2.1 | 0.06; 0.009 | 211; 66 |
| 44 | >32 | 10,090 | 3550 | 2.8 | 0.06; 0.010 | 575; 267 |

^a Concentrations reported at MED except for **44** (17.8 mg/kg).

^b Minimal effective dose; compounds were formulated in 5:5:90 DMSO/cremophor/saline; animals sacrificed at 2 h post dose except for **40** (30 min post dose); brain and plasma levels analyzed.

^c Fraction unbound in mouse plasma and brain.

^d [Plasma]_{free} = [plasma] × Fu_p; [brain]_{free} = [brain] × Fu_b.

Table 3
Human 5-HT_{2A} binding activity

| Compounds | h 5-HT _{2A} (K _i , nM) | Compounds | h 5-HT _{2A} (K _i , nM) |
|-----------|--|-----------|--|
| 17 | >3200 | 40 | 323 |
| 38 | 2100 | 44 | >3100 |
| 39 | >3100 | 46 | >3100 |

containing a pyridyl nitrogen in place of phenyl (**44** and **46**) had much weaker 5-HT_{2A} binding activity (Table 3).

Compounds **38**, **40** and **44**, as well as the mGluR2 agonist, LY354740⁴, were evaluated in an anti-psychosis model, testing a compound's ability to attenuate methamphetamine-induced hyperlocomotor activity in mice.²⁴ The mGluR2 agonist showed significant activity at 0.01 mg/kg, s.c., whereas the mGluR2 PAMs, **38** and **40**, required a minimal effective dose (MED) of 10 mg/kg, s.c. At the MED dose, compounds **38** and **40** had free plasma exposures of 33 and 211 nM, respectively, and brain/plasma ratios >2 (see Table 4). To determine the amount of free drug in the brain

Table 5
Pharmacokinetic data in rats.

| Compounds | CLp (mL/min/kg) ^a | Vdss (L/kg) | T _{1/2} (h) | %F ^b |
|-----------|------------------------------|-------------|----------------------|-----------------|
| 38 | 102 | 3.2 | 0.8 | 64 |
| 44 | 18.1 | 4.7 | 3.8 | 100 |

^a 1 mg/kg iv dose.

^b F based on oral dose of 10 mg/kg **38** and 3 mg/kg **44**.

([brain]_{free}), the unbound fractions in mouse brain (Fu_b) were measured. The [brain]_{free} of **38** (2 h post dose) and **40** (0.5 h post dose) at the MED were calculated to be 34 and 66 nM, respectively, similar to their in vitro EC₅₀ values (30 and 70 nM, respectively). However, for compound **40** it is unclear how much of its activity in the locomotor assay is due to 5-HT_{2A}, or whether 5-HT_{2A} activity could act synergistically with mGluR2 in this model.²⁵ Compound **44** was not active at doses up to 32 mg/kg, likely reflecting the larger hurdle of covering a less potent EC₅₀ of 380 nM. Finally, compounds **38** and **44** were both shown to have good oral bioavailability in rats (Table 5); and **44** had low plasma CL and a moderate half-life (T_{1/2} = 3.8 h). Compound **38**, however, appeared to have high clearance (CL = 102 mL/min/kg, undefined explanation), suggestive of extrahepatic metabolism, and a moderate volume (4.7 L/kg), resulting in a short half-life (0.8 h). It is noteworthy that in the presence of rat liver microsomes, compound **38** had a relatively high in vitro CL of 51 mL/min/kg.

In summary, we have identified a promising new series of mGluR2 PAMs, characterized by high brain penetration and good ligand efficiency. This work highlighted the importance of a thorough hit assessment process as part of the hit-to-lead paradigm. Judicious library design allowed to reach a decision making point on this series in one iteration of synthesis. Modification of the alkylether moiety of **17** led to a series of biaryl analogs with lower human microsomal CL and improved physical properties (**38–40**). Efforts to introduce polar functionality and/or an ionizable center were successful in that they improved solubility, reduced cLogP, provided a salt handle and lowered human microsomal CL, but these compounds had generally less potent mGluR2 PAM activity. Compound **38** was found to be active in an in vivo methamphetamine-induced hyperlocomotor model at a free brain exposure nearly equal to its in vitro mGluR2 PAM EC₅₀ of 30 nM, but the total plasma exposure required to achieve this was high (2.3 μM) due to high protein binding. We conclude that future endeavors will have to address the high lipophilicity seemingly required for mGluR2 PAM binding in the transmembrane domain versus the reduced lipophilicity necessary for lower protein binding.

Acknowledgments

The authors thank Bruce Posner and Csilla Csiki Jorgensen for the HTS work, Jon Bordner for the single crystal X-ray structure elucidation of compound **3**, Joel Schachter and Diane Lang for constructing cells and Professor Shigetada Nakanishi of Kyoto University for providing cDNA. We also thank Rebecca O'Connor and Anne

Schmidt for 5-HT_{2A} data, Elaine Tseng for exposure data for compound **40**, Dianne Wong for generating B/P data for compound **17**, and our ADME technology group for microsomal clearance data.

References and notes

- Pin, J.-P.; Galvez, T.; Prezeau, L. *Pharmacol. Ther.* **2003**, *98*, 325.
- Poisik, O.; Raju, D. V.; Verreault, M.; Rodriguez, A.; Abeni, O. A.; Conn, P. J.; Smith, Y. *Neuropharmacology* **2005**, *49*, 57.
- Kew, J. N. C.; Kemp, J. A. *Psychopharmacology* **2005**, *179*, 4.
- Grillon, C.; Cordova, J.; Levine, L. R. *Psychopharmacology* **2003**, *168*, 446.
- Rorick-Kehn, L. M.; Johnson, B. G.; Knitowski, K. M.; Salhoff, C. R.; Witkin, J. M.; Perry, K. W.; Griffey, K. I.; Tizzano, J. P.; Monn, J. A.; McKinzie, D. L.; Schoepp, D. D. *Psychopharmacology* **2007**, *193*, 121.
- Marek, G. J. *Curr. Opin. Pharmacol.* **2004**, *4*, 18.
- Linden, A.-M.; Schoepp, D. D. *Drug Discovery Today: Therapeutic Strategies* **2006**, *3(4)*, 507.
- Patil, S. T.; Zhang, L.; Martenyi, F.; Lowe, S. L.; Jackson, K. A.; Andreev, B. V.; Avedisova, A. S.; Bardenstein, L. M.; Gurovich, I. Y.; Morozova, M. A.; Mosolov, S. N.; Neznanov, N. G.; Reznik, A. M.; Smulevich, A. B.; Tochilov, V. A.; Johnson, B. G.; Monn, J. A.; Schoepp, D. D. *Nat. Med.* **2007**, *13*, 1102.
- For a review, see: Rudd, M. T.; McCauley, J. A. *Curr. Top. Med. Chem.* **2005**, *5*, 869.
- Zhang, L.; Rogers, B. N.; Duplantier, A. J.; McHardy, S. F.; Efremov, I.; Berke, H.; Qian, W.; Zhang, A. Q.; Maklad, N.; Candler, J.; Doran, A. C.; Lazzaro, J. T., Jr.; Ganong, A. H. *Bioorg. Med. Chem. Lett.* **2008**, *18*, 5493.
- Recasens, M.; Guiramand, J.; Aimar, R.; Abdulkarim, A.; Barbanel, G. *Curr. Drug Targets* **2007**, *8*, 651.
- Gjoni, T.; Urwyler, S. *Neuropharmacology* **2008**, *55*, 1293.
- (a) Goodnow, R. A., Jr.; Gillespie, P. *Prog. Med. Chem.* **2007**, *45*, 1; (b) Wunberg, T.; Hendrix, M.; Hillisch, A.; Lobell, M.; Meier, H.; Schmeck, C.; Wild, H.; Hinzen, B. *Drug Discovery Today* **2006**, *11*, 175; (c) Keseru, G.; Makara, G. *Drug Discovery Today* **2006**, *11*, 741; (d) Alanine, A.; Nettekoven, M.; Roberts, E.; Thomas, A. W. *Comb. Chem. High Throughput Screen.* **2003**, *6*, 51.
- MS-based quantification of the basal/apical transfer rate of a test compound at 2 μM across contiguous monolayers from MDCK (Madin Darby Canine Kidney) cells.
- Ratio from the MS-based quantification of apical/basal and basal/apical transfer rates of a test compound at 2 μM across contiguous monolayers from MDR1-transfected MDCK cells.
- Hopkins, A. L.; Groom, C. R.; Alexander, A. *Drug Discovery Today* **2004**, *9*, 430.
- Ligand efficiency is calculated based on binding affinity. Since the mGluR2 assay used is a functional assay and the EC₅₀ value depends on the concentration of glutamate present in the assay, the precise assessment of the ligand efficiency based on this assay was not possible. At the same time, comparison of LE profiles of multiple chemotypes using the same mGluR2 assay provided a valuable perspective when assessing lead generation potential of different chemical series.
- Hitchcock, S. A. *Curr. Opin. Chem. Biol.* **2008**, *12*, 318.
- (a) Patel, Y.; Gillet, V. J.; Howe, T.; Pastor, J.; Oyarzabal, J.; Willett, P. J. *Med. Chem.* **2008**, *51*, 7552; (b) Dill, K. A. J. *Biol. Chem.* **1997**, *272*, 701.
- Feng, B.; Mills, J. B.; Davidson, R. E.; Mireles, R. J.; Janiszewski, J. S.; Troutman, M. D.; de Morais, S. M. *Drug Metab. Dispos.* **2008**, *36*, 268.
- Fluorescence-based measurement of CYP inhibition by incubating the recombinant CYP (Cytochrome P450) with a test compound and the corresponding fluorescent probe at 3 μM.
- Scintillation proximity assay measuring inhibition of ³H-dofetilide binding to membranes from hERG-expressing HEK cells at 10 μM.
- In efforts to obtain analogs in solid form, we compared the MPs of small alkoxyphenyl ethers (oils) to benzylphenyl ether (~40 °C), phenyl ether (~28 °C) and biphenyl (~70 °C).
- (a) Hirota, S.; Kawashima, N.; Chaki, S.; Okuyama, S. *CNS Drug Rev.* **2003**, *9(4)*, 375; (b) Satow, A.; Maehara, S.; Ise, S.; Hikichi, H.; Fukushima, M.; Suzuki, G.; Kimura, T.; Tanaka, T.; Ito, S.; Kawamoto, H.; Ohta, H. *J. Pharmacol. Exp. Ther.* **2008**, *326*, 577.
- Gonzalez-Maeso, J.; Ang, R. L.; Yuen, T.; Chan, P.; Weisstaub, N. V.; Lopez-Gimenez, J. F.; Zhou, M.; Okawa, Y.; Callado, L. F.; Milligan, G.; Gingrich, J. A.; Filizola, M.; Meana, J. J.; Sealfon, S. C. *Nat. Lett.* **2008**, *1*.